Nanotechnology **18** (2007) 195103 (6pp) doi:10.1088/0957-4484/18/19/195103

Isolation of carbon nanohorn assemblies and their potential for intracellular delivery

Xiaobin Fan[1], **Juan Tan**[2], **Guoliang Zhang**[1] **and Fengbao Zhang**[1]

[1] School of Chemical Engineering and Technology, Tianjin University, Tianjin, People's Republic of China
[2] College of Life Sciences, Nankai University, Tianjin, People's Republic of China

E-mail: fbzhang@tju.edu.cn

Received 10 February 2007, in final form 14 March 2007
Published 17 April 2007
Online at stacks.iop.org/Nano/18/195103

Abstract
Attributed to its distinctive dahlia-flowerlike structure and already desirable size (usually <100 nm), carbon nanohorn assemblies (CNHs), a new member of the fullerene family, are a potential vehicle for intracellular delivery. This paper shows that isolated CNHs and nanoscale CNH agglomerates can be successfully isolated by a copolymer (Gum Arabic) through steric stabilization. *In vitro* study shows that the modified CNHs are nontoxic and may be used as a promising vehicle for intracellular delivery.

1. Introduction

Integrating nanotechnology with biology and medicine has attracted increasing attention. In particular, because of their dimensional similarities to biomolecules, many inorganic nanoscopic materials are under intensive investigation as synthetic delivery vehicles (Chen *et al* 2005, Hong *et al* 2006, Kam *et al* 2005, Kohler *et al* 2005, Pantarotto *et al* 2004, Tkachenko *et al* 2003). Carbon nanohorn (CNH) is a recently recognized member of the fullerene family (Iijima *et al* 1999). A single CNH has a structure similar to a pudgy single-wall carbon nanotube (SWCNT) (Iijima and Ichihashi 1993) with one end closed in a cone-shaped cap (horn). Due to strong van der Waals forces, CNHs form spherical dahlia-flowerlike assemblies. This distinctive structure may gives CNHs potential advantages over normal nanoparticles, nanorods and nanotubes for intracellular delivery. For instance, meticulous cutting is unnecessary for CNHs because of their already desirable sizes (usually <100 nm). In addition, sphere-shaped nanoparticles with moderate size show improved cellular uptake efficiency over their rod-shaped counterparts (Chithrani *et al* 2006). Further, compared with common nanoparticles, CNHs have larger surface areas and more cavities (Iijima *et al* 1999, Murata *et al* 2000) to absorb and hold therapeutic drugs, genes or proteins. Two drugs (cisplatin and dexamethasone) have already been successfully incorporated into CNHs to achieve ideal controlled releases (Ajima *et al* 2005, Murakami *et al* 2004). However, their insolubility in water and their great tendency to agglomerate (micrometre-order) restrict their extensive use in biological applications, especially in intracellular delivery. Recently, covalent functionalization of CNHs with cationic ammonium to improve their solubility has been reported (Tagmatarchis *et al* 2006), but still leaving the aggregating feature behind.

In this paper, we introduce an easy and effective method to isolate CNHs, and evaluate the potential of CNHs as intracellular vehicles.

2. Experimental details

2.1. Isolation of CNH assemblies

Gum Arabic (GA, Aldrich, 10 g) was dissolved in 100 ml deionized water to achieve a transparent GA solution. Then, 20 ml of the above GA solution was added to a beaker containing untreated CNHs (Nanocraft, Inc., up to 0.2 g). The mixture was sonicated (120 W, 40 kHz, 20 min) in an ice water bath to achieve a homogeneous black suspension. Modified CNHs can be obtained by centrifugation (>12 000 g) or drying the suspension at room temperatures.

2.2. Covalent linkage of rhodamine B with GA

GA (2 g) was dissolved in 20 ml 0.1 M 2-[*N*-morpholino] ethane sulfonic acid buffer (MES, Sigma) to get solution A.

 © 2007 IOP Publishing Ltd Printed in the UK

Then, 45 mg rhodamine B (RhB, Sigma) was dissolved in 1 ml 0.1 M MES to get solution B. Directly after adding solution B to solution A, a fresh 1-ethyl-3-(3-dimethylaminopropyl) carbodiimide hydrochloride (EDC, Fluka) solution (25 mg in 1 ml deionized water) was added to the mixture above. This coupled the amine groups (GA) with carboxyl groups (RhB) for 2 h at room temperature. The RhB–GA complex was purified by dialyzing for 3 d.

2.3. Preparation of RhB–GA–CNHs

Untreated CNHs (500 mg) were dispersed in the RhB–GA complex above (5 ml) by sonication in an ice water bath. The unsuspended CNHs were removed by centrifugating at 12 000 g for 30 min. Then, the supernatant was centrifuged again (250 000 g, 1 h) to precipitate the RhB–GA–CNHs conjugate. The obtained precipitate was redispersed in 5 ml Dulbecco's modified eagle's medium (DMEM) for intracellular delivery.

2.4. Cytotoxicity

HeLa cells were cultured in DMEM containing 10% foetal bovine serum (FBS) at 37 °C with 5% CO_2. The cells were seeded on a 96-well plate with the density of about 1×10^4 cells a well. After 24 h incubation, the culture media was replaced with fresh media containing modified CNHs with various dosages (0.01–1 mg ml^{-1}). After incubation at 37 °C for 8 h, the CNHs-containing media were replaced with fresh media for later (24 h) cell viability analysis by performing the 3-(4,5-dimethylthiazol-2-yl)-2,5-diphenyl-tetrazolium bromide (MTT, Sigma) assay (Mosmann 1983). Cells incubated in DMEM lacking CNHs were used as control.

2.5. Internalization of CNHs and RhB–GA–CNHs

The cells seeded on the 12-well plate were incubated with modified CNHs (80 μl, 1 mg ml^{-1}) or the RhB–GA–CNHs conjugate (80 μl) in a serum-free DMEM culture (120 μl) at 37 °C for 4–7 h. After the incubation, the cells were washed with phosphate-buffer saline (PBS, Sigma) five times to remove CNHs or RhB–GA–CNHs conjugate for observation. To stain the nucleus of cells, the cells were fixed 15 min with 4% paraformaldehyde (Sigma-Aldrich), rehydrated in PBS for three times, stained with 300 nM DAPI (Invitrogen) for 8 min and washed with PBS for three times.

2.6. Characterization

SEM measurements were carried out on an FE-SEM (JSM-6700F, JEOL). XPS spectra were collected with a PHI 1600 spectrometer (Perkin–Elmer). Raman spectroscopy was performed by a Renishaw inVia Raman microscope with the excitation wavelength of 514.5 nm. HRTEM micrographs were taken on an FEI Tecnai G2 F20 microscope. The optical density of formazan for MTT assay was measured at 570 nm using a Multiskan Ascent plate reader. The fluorescence microscopy was performed on an Olympus IX71 microscope equipped with an SPOT RT digital camera.

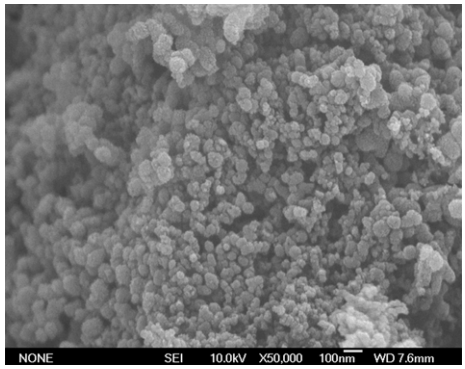

Figure 1. Typical SEM image of untreated CNHs.

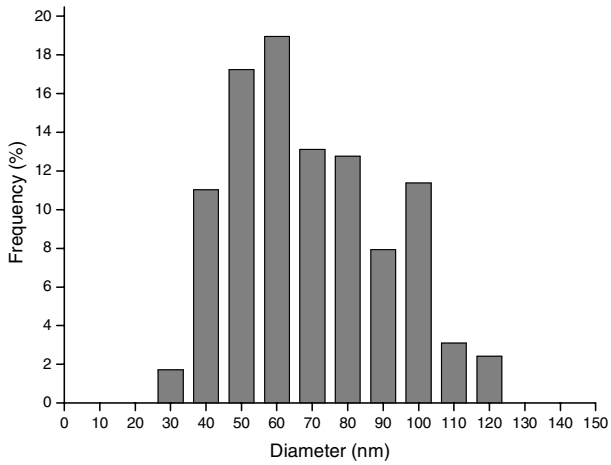

Figure 2. Size distribution of untreated CNHs calculated from figure 1.

3. Results and discussion

3.1. Theory

Scanning electron microscopy (SEM, figure 1) shows the untreated CNHs have a broad size distribution of 30–120 nm (figure 2) and attract one another due to van der Waals forces. According to Hamaker's theory (Hamaker 1937, Israelachvili 1992), the nonretarded energy and van der Waals force between two CNHs of volumes V_1 and V_2 containing q_1 and q_2 atoms per cm^3 are:

$$W = -\int_{V_1} \mathrm{d}v_1 \int_{V_2} \mathrm{d}v_2 \frac{q_1 q_2 \lambda_{1,2}}{D^6} \tag{1}$$

$$F = \frac{\partial W}{\partial D} \tag{2}$$

where D is the separation distance and $\lambda_{1,2}$ is London's constant for C–C. For two spherical CNHs of radii R_1 and R_2:

$$F = \frac{-A}{6D^2}\left(\frac{R_1 R_2}{R_1 + R_2}\right) \tag{3}$$

where A is the effective Hamaker constant of CNHs and is defined as follows:

$$A = \pi^2 q_1 q_2 \lambda_{1,2}. \tag{4}$$

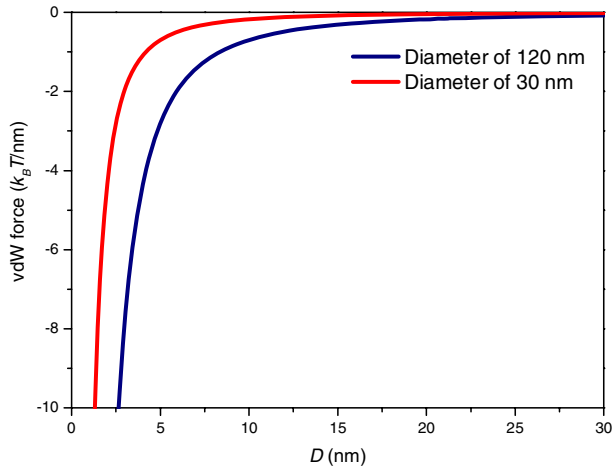

Figure 3. The van der Waals forces between two CNHs as a function of separation.

Under the assumption the porous materials can be treated as a continuum with homogeneous porosity, their atomic densities can be derived from their condensed counterpart:

$$q_{(\text{porous})} = (1-\varepsilon)q_{(\text{condensed})} \tag{5}$$

$$\varepsilon = \frac{V_{\text{void}}}{V_{\text{void}} + V_{\text{solid}}} \tag{6}$$

where ε is the porosity (the percentage of the void volume) of the porous material, V_{solid} is the solid volume and V_{void} is the void volume. Since $(1-\varepsilon)^2$ can be taken out directly from the integrals in equation (1), the unknown Hamaker constant of a CNH assembly can be derived from its condensed counterpart (graphite) by treating the CNH assembly as a porous sphere with a uniform density distribution:

$$A_{\text{CNHs}} \approx (1-\varepsilon)^2 A_{\text{Graphite}}. \tag{7}$$

According to the geometric model of CNHs (Murakami *et al* 2004), V_{void} includes the open pore volume V_{op}, the closed pore volume V_{cp} and the latent pore volume V_{lp}. Therefore, a value of 0.58 for the ε can be obtained according to equation (6). About the Hamaker constant of graphite in air, a theoretical value of 2.53×10^{-19} J (Dagastine *et al* 2002) was used in this study. Thus, the Hamaker constant of CNHs in air is estimated to be about 0.58×10^{-19} J. According to equation (3), the van der Waals forces between two CNHs (figure 3) approach zero when their separation is larger than 15 and 25 nm (for the smallest and largest CNHs, respectively). This result means that a thermodynamically stable suspension of isolated CNHs can be formed through steric stabilization by various copolymers (Napper 1993).

3.2. Isolation of CNHs

We use Gum Arabic (GA) (Bandyopadhyaya *et al* 2002, Islam *et al* 1997) as a typical copolymer in this study, because it is biocompatible and its protein moieties can be conjugated with biological cargoes for intracellular delivery. As shown in figure 4(a), during mild sonication, the hydrophobic polypeptide chains of GA will spontaneously

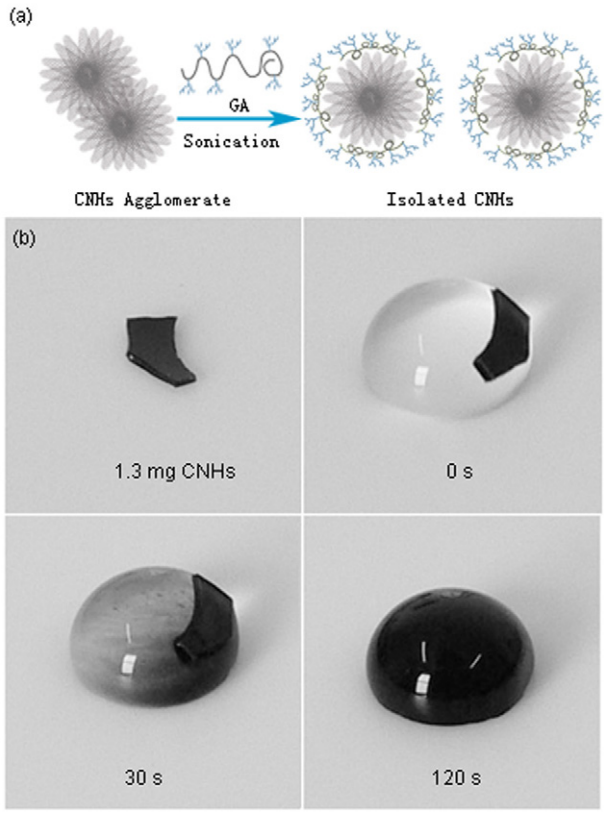

Figure 4. Illustration for the isolation of CNHs using GA (a) and the spontaneous dissolution of modified CNHs (b).

adsorb onto the surface of temporarily isolated CNHs, while the hydrophilic arabinogalactan polysaccharide sidechains extend into the water providing a steric barrier (Islam *et al* 1997). Homogeneous ink-like CNHs suspensions prepared with this approach are stable for at least 6 months. The thermodynamical stability of the suspensions was confirmed by the spontaneous redispersion of modified CNHs in water (figure 4(b)), a signature of steric stabilization (Napper 1993).

Raman spectra (figure 5) show the modified CNHs have a slight increase in the intensity of the disorder-induced mode (D-band). This result means the sonication conditions (120 W, 40 kHz, 20 min in an ice water bath) only cause mild damage of the CNHs. The slight upshift (6 cm^{-1}) of the tangential mode (G-band) indicates compressive strain on CNHs after modification (Liu *et al* 2005), due to the strong attachment of GA to the CNHs. The presence of GA is further confirmed by the x-ray photoelectron spectroscopy (XPS). The XPS spectrum of modified CNHs (figure 6) shows a new peak at 399 eV for N 1s and an increase in the atomic ratio of O to C from 0.116 to 0.411. High-resolution C 1s spectra (data nor shown) not only show a significant increase for the C=O bonds (288.2 eV), but also display a new peak at 286.4 for the C–O and C–N bonds of GA. These results clearly show that GA attaches to the surface of the CNHs.

The separation of the CNH agglomerates by GA was verified by high resolution transmission electron microscopy (HRTEM). As seen from figure 7(a), the surface of individual CNHs is covered by a GA layer which provides steric stabilization. Besides isolated CNHs, small agglomerates are

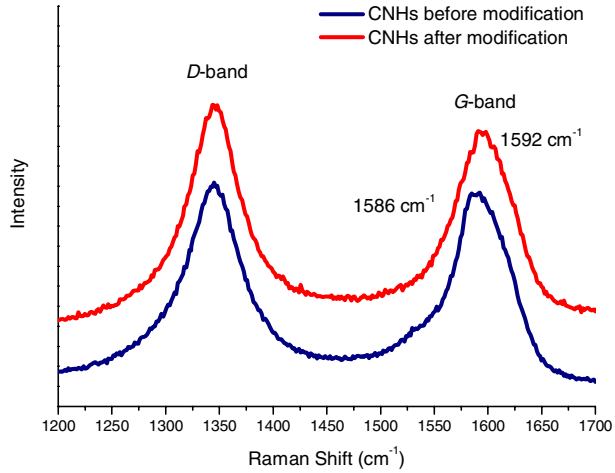

Figure 5. Raman spectra of CNHs before (blue) and after modification (red).

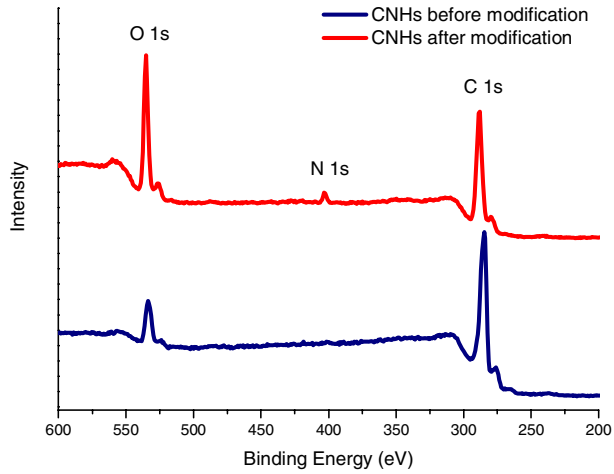

Figure 6. XPS spectra of CNHs before (blue) and after modification (red).

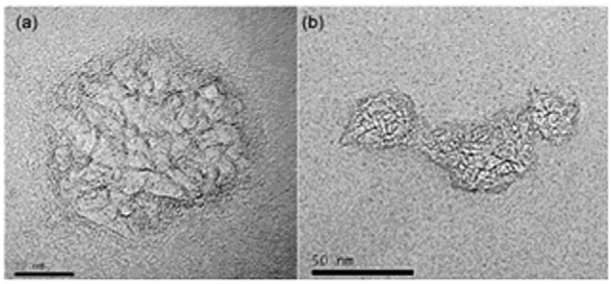

Figure 7. Typical HRTEM images of CNHs after modification. The scale bar in (a) and (b) are 10 and 50 nm, respectively.

also observed in the CNHs suspensions (figure 7(b)). These small agglomerates are formed by bridging two or more assemblies with common polypeptide chains (GA) (Napper 1993). Interestingly, the relatively large assemblies (80–120 nm) which are plentiful in the untreated CNHs are rare in the final suspension. Thus, the small agglomerates here

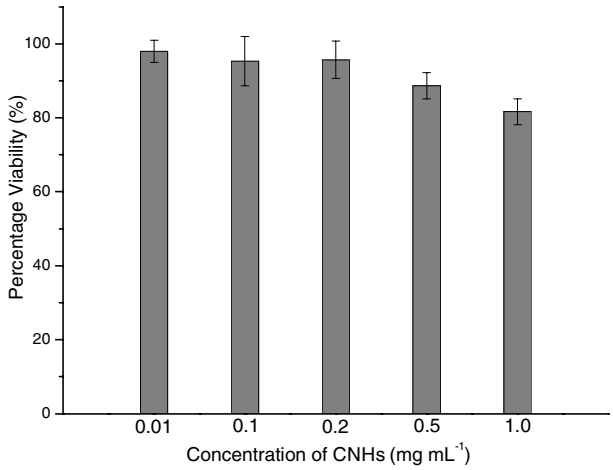

Figure 8. Cytotoxicity of modified CNHs when incubated with HeLa cells as determined by MTT assay ($n = 3$).

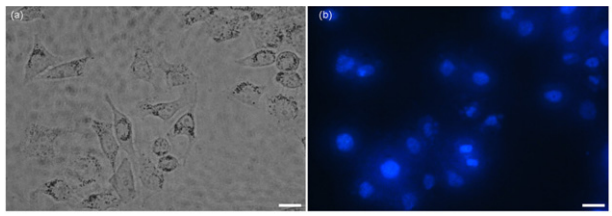

Figure 9. Light microscopy image (a) of HeLa cells after incubation with modified CNHs and corresponding fluorescent image (b) of the nucleus stained by DAPI. The black spots in (a) show the perinuclear accumulation of CNHs. The scale bars are 20 μm.

probably come from the separation of a large assembly. Similar results can be found in a previous study using a surfactant of sodium dodecylbenzene sulfonate (Zhang *et al* 2005).

3.3. Cytotoxicity

Studies of the cytotoxicity of CNHs were performed by incubating modified CNHs with human cervical cancer cells (HeLa cells) for 8 h in a DMEM culture containing serum. Cell viability analysis (MTT assay) (Mosmann 1983) after 24 h showed that more than 80% of the cells remained viable even with CNHs' concentrations up to 1 mg ml^{-1} (figure 8), and no obvious decrease of the cell viability was observed with time getting longer (48 and 72 h later). This result means the modified CNHs are nontoxic. High purity CNHs can be prepared without the use of metallic catalysts which accounts for most the cytotoxicity of carbon nanotubes (Shvedova *et al* 2003). Thus CNHs have superior biocompatibility. Besides, the surface modification of CNHs with the natural polysaccharide may also improve the biocompatibility.

3.4. Intracellular delivery

To probe the ability of CNHs to enter cells, CNHs were incubated with HeLa cells in a serum-free DMEM culture. After 4–7 h of incubation, most of the CNHs (in the black vesicles) were found in the perinuclear regions of the cells (figures 9(a) and (b)), which is mainly occupied by the late

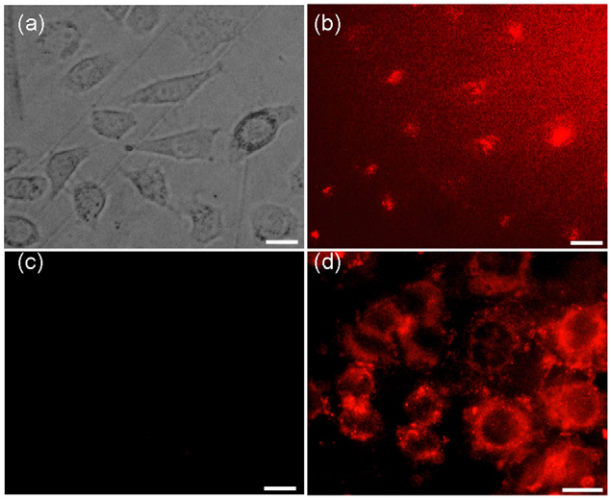

Figure 10. The light (a) and fluorescent images (b) of the HeLa cells after incubation with RhB–GA–CNHs conjugate, and fluorescent images of control without RhB–GA–CNHs conjugate (c) and with RhB–GA conjugate (d). The incubation time for both the RhB–GA and RhB–GA–CNHs conjugate is 7 h. The red fluorescent background in (b) is attributed to the autocompensation by the microscope due to the weak fluorescent signals from the cells. The scale bars are 20 μm.

endosome or lysosome. No CNHs locates in the nucleus of the cells, suggesting that CNHs do not enter the nucleus. This result is expected since it would be difficult for CNHs to permeate through the channels of the nuclear pore complex (NPC, diameter of <40 nm), which serves as the gateway for nucleo-cytoplasmic transport (Fahrenkrog and Aebi 2003). Endocytosis of cells is a widely accepted mechanism for the internalization of nanoparticles. A series of detailed experiments should be carried out to confirm this pathway. The fast perinuclear accumulation of CNHs suggests that they may be used as an efficient intracellular vehicle for biological cargoes.

We speculated that a biological cargo could link to GA and be delivered by CNHs. To test this feasibility, rhodamine B (RhB) was covalently linked to the polypeptide chain of GA with the presence of EDC. The fluorescent RhB–GA conjugate was then used to evaluate the delivery efficiency of CNHs. Light microscopy in figure 10(a) shows the uptake of CNHs conjugates by the cells and their distribution around the cell's nucleus. Surprisingly, although the fluorescent signals are weak, corresponding fluorescent microscopy (figure 10(b)) reveals that they are emitted from the nucleus of the cells and not from the region in which the CNHs gather. On the contrary, negative control (figure 10(c)) with DMEM lacking the RhB–GA–CNHs conjugate shows no fluorescent signal, as expected. Please note that RhB is a fluorescent dye that selectively stains the mitochondria of cells, and a repeated control experiment with RhB–GA conjugate resulted in a clear non-nuclear location of the fluorescent signals. Probably due to the exposure of RhB in the RhB–GA conjugate, the RhB–GA conjugates will be retained by the mitochondria in the cytoplasm, and RhB cannot be delivered into the nucleus by GA alone (figure 10(d)). Based on these results, we believed the RhB molecules which were covalently linked to the polypeptide chains of GA were protected by the outermost polysaccharide layer on the isolated CNHs (figure 4(a)). Thus, after being delivered to or near the nuclear envelope by the CNHs, the RhB separated (due to the degradation of the polypeptide chain) from the CNHs and then diffused through the NPC into the nucleus. However, further studies should be carried out to clarify the mechanism involved.

4. Conclusions

In summary, CNH agglomerates can be successfully isolated by attaching GA to achieve a stable suspension through steric stabilization. The modified CNHs show excellent biocompatibility because of their high purity and the surface modification of GA. *In vitro* studies confirm that CNHs can readily enter the cells, probably through the endocytic pathway. Notably, CNHs shows great potentials as intracellular delivery vehicles for various biomolecules.

References

Ajima K, Yudasaka M, Murakami T, Maigne A, Shiba K and Iijima S 2005 Carbon nanohorns as anticancer drug carriers *Mol. Pharm.* **2** 475–80

Bandyopadhyaya R, Nativ-Roth E, Regev O and Yerushalmi-Rozen R 2002 Stabilization of individual carbon nanotubes in aqueous solutions *Nano Lett.* **2** 25–8

Chen C C, Liu Y C, Wu C H, Yeh C C, Su M T and Wu Y C 2005 Preparation of fluorescent silica nanotubes and their application in gene delivery *Adv. Mater.* **17** 404–7

Chithrani B D, Ghazani A A and Chan W C 2006 Determining the size and shape dependence of gold nanoparticle uptake into mammalian cells *Nano Lett.* **6** 662–8

Dagastine R R, Prieve D C and White L R 2002 Calculations of van der Waals forces in 2-dimensionally anisotropic materials and its application to carbon black *J. Colloid Interface Sci.* **249** 78–83

Fahrenkrog B and Aebi U 2003 The nuclear pore complex: nucleocytoplasmic transport and beyond *Nat. Rev. Mol. Cell. Biol.* **4** 757–66

Hamaker H C 1937 The London–van der Waals attraction between spherical particles *Physica* **4** 1058–72

Hong R, Han G, Fernandez J M, Kim B J, Forbes N S and Rotello V M 2006 Glutathione-mediated delivery and release using monolayer protected nanoparticle carriers *J. Am. Chem. Soc.* **128** 1078–9

Iijima S and Ichihashi T 1993 Single-shell carbon nanotubes of 1 nm diameter *Nature* **363** 603–5

Iijima S, Yudasaka M, Yamada R, Bandow S, Suenaga K and Kokai F 1999 Nano-aggregates of single-walled graphitic carbon nano-horns *Chem. Phys. Lett.* **309** 165–70

Islam A M, Phillips G O, Sljivo A, Snowden M J and Williams P A 1997 A review of recent developments on the regulatory, structural and functional aspects of gum arabic *Food Hydrocoll.* **11** 493–505

Israelachvili J 1992 *Intermolecular and Surface Forces* (San Diego, CA: Academic)

Kam N W, Liu Z and Dai H 2005 Functionalization of carbon nanotubes via cleavable disulfide bonds for efficient intracellular delivery of siRNA and potent gene silencing *J. Am. Chem. Soc.* **127** 12492–3

Kohler N, Sun C, Wang J and Zhang M Q 2005 Methotrexate-modified superparamagnetic nanoparticles and their intracellular uptake into human cancer cells *Langmuir* **21** 8858–64

Liu J, Liu T and Kumar S 2005 Effect of solvent solubility parameter on SWNT dispersion in PMMA *Polymer* **46** 3419–24

Mosmann T 1983 Rapid colorimetric assay for cellular growth and survival: application to proliferation and cytotoxicity assays *J. Immunol. Methods* **65** 55–63

Murakami T, Ajima K, Miyawaki J, Yudasaka M, Iijima S and Shiba K 2004 Drug-loaded carbon nanohorns: adsorption and release of dexamethasone *in vitro Mol. Pharm.* **1** 399–405

Murata K, Kaneko K, Kokai F, Takahashi K, Yudasaka M and Iijima S 2000 Pore structure of single-wall carbon nanohorn aggregates *Chem. Phys. Lett.* **331** 14–20

Napper D H 1993 *Polymeric Stabilization of Colloidal Dispersions* (Orlando, FL: Academic)

Pantarotto D, Briand J P, Prato M and Bianco A 2004 Translocation of bioactive peptides across cell membranes by carbon nanotubes *Chem. Commun.* 16–7

Shvedova A A, Castranova V, Kisin E R, Schwegler-Berry D, Murray A R, Gandelsman V Z, Maynard A and Baron P 2003 Exposure to carbon nanotube material: assessment of nanotube cytotoxicity using human keratinocyte cells *J. Toxicol. Environ. Health* A **66** 1909–26

Tagmatarchis N, Maigne A, Yudasaka M and Iijima S 2006 Functionalization of carbon nanohorns with azomethine ylides: towards solubility enhancement and electron-transfer processes *Small* **2** 490–4

Tkachenko A G, Xie H, Coleman D, Glomm W, Ryan J, Anderson M F, Franzen S and Feldheim D L 2003 Multifunctional gold nanoparticle–peptide complexes for nuclear targeting *J. Am. Chem. Soc.* **125** 4700–1

Zhang M, Yudasaka M, Miyawaki J, Fan J and Iijima S 2005 Isolating single-wall carbon nanohorns as small aggregates through a dispersion method *J. Phys. Chem.* B **109** 22201–4